Supplementary Information (SI) for Inorganic Chemistry Frontiers.

Crosslinked Ion-conducting Hybrid Coating Layers for Robust Artificial Solid-electrolyte Interphase Towards High-Performance Silicon Anodes

Yuhui Weng[ab], *Xingyu Sun*[a], *Siying Li*[a], *Zhuoying Wu*[a], *Ziwei Chen*[ab], *Yongqun Ma*[ab], *Zefan Zheng*[ab], *Feng Lin*[c], *Ming Zhang*[d], *Kejun Zhang*[e], *Min Ling*[*a], *Keli Yang*[*f], *Chengdu Liang*[*a], *Jun Chen*[*ab].

a Zhejiang Provincial Key Laboratory of Advanced Chemical Engineering Manufacture Technology, College of Chemical and Biological Engineering, Yu Hang Tong Road 866，Zhejiang University, Hangzhou 310027, China.

b Institute of Zhejiang University-Quzhou, Zheda Road 99, Quzhou 324000, China.

c College of Chemical and Materials Engineering, Quzhou University, Quzhou, 324000, China

d Quzhou Jingzhou Technology Development Co., Ltd, Quzhou, 324000, China.

e Huayou New Energy Technology (Quzhou) Co., Ltd, Quzhou, 324000, China.

f Key Laboratory of Green and High-end Utilization of Salt Lake Resources, Qinghai Institute of Salt Lakes, Chinese Academy of Sciences, Beijing, 100864, China.

* Corresponding author. E-mail address: Minling@zju.edu.cn (Min Ling); yangkl@isl.ac.cn (Keli Yang); cdliang@zju.edu.cn (Chengdu Liang); qiujinchen@zju.edu.cn (Jun Chen).

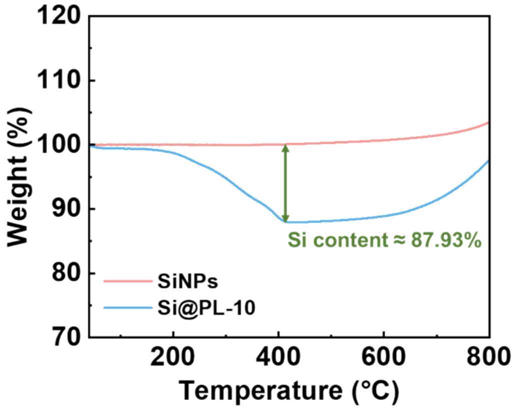

Fig. S1. TGA curves of Si@PL-10 and SiNPs

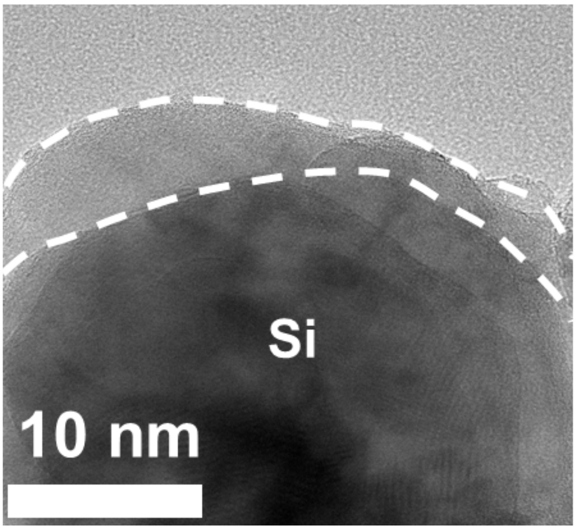

Fig. S2 HRTEM image of Si@PAA particles.

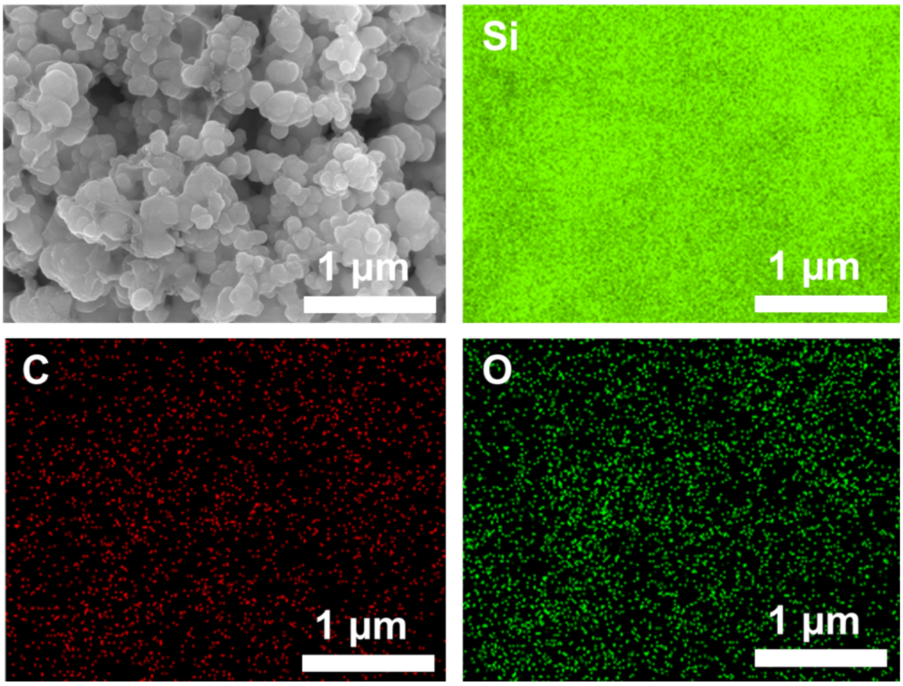

Fig. S3. SEM image of Si@PL-10 particles and the corresponding EDS Mapping results.

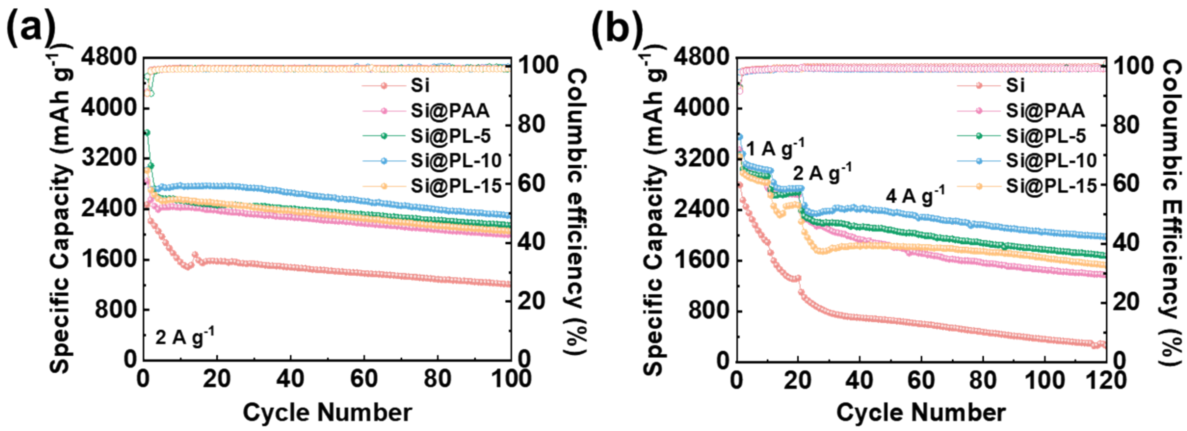

Fig. S4. (a) Cycling performance and Coulombic efficiency of different Si electrodes at 2 A g^{-1}. (b) Cycling performance and Coulombic efficiency of different Si electrodes at 4 A g^{-1}.

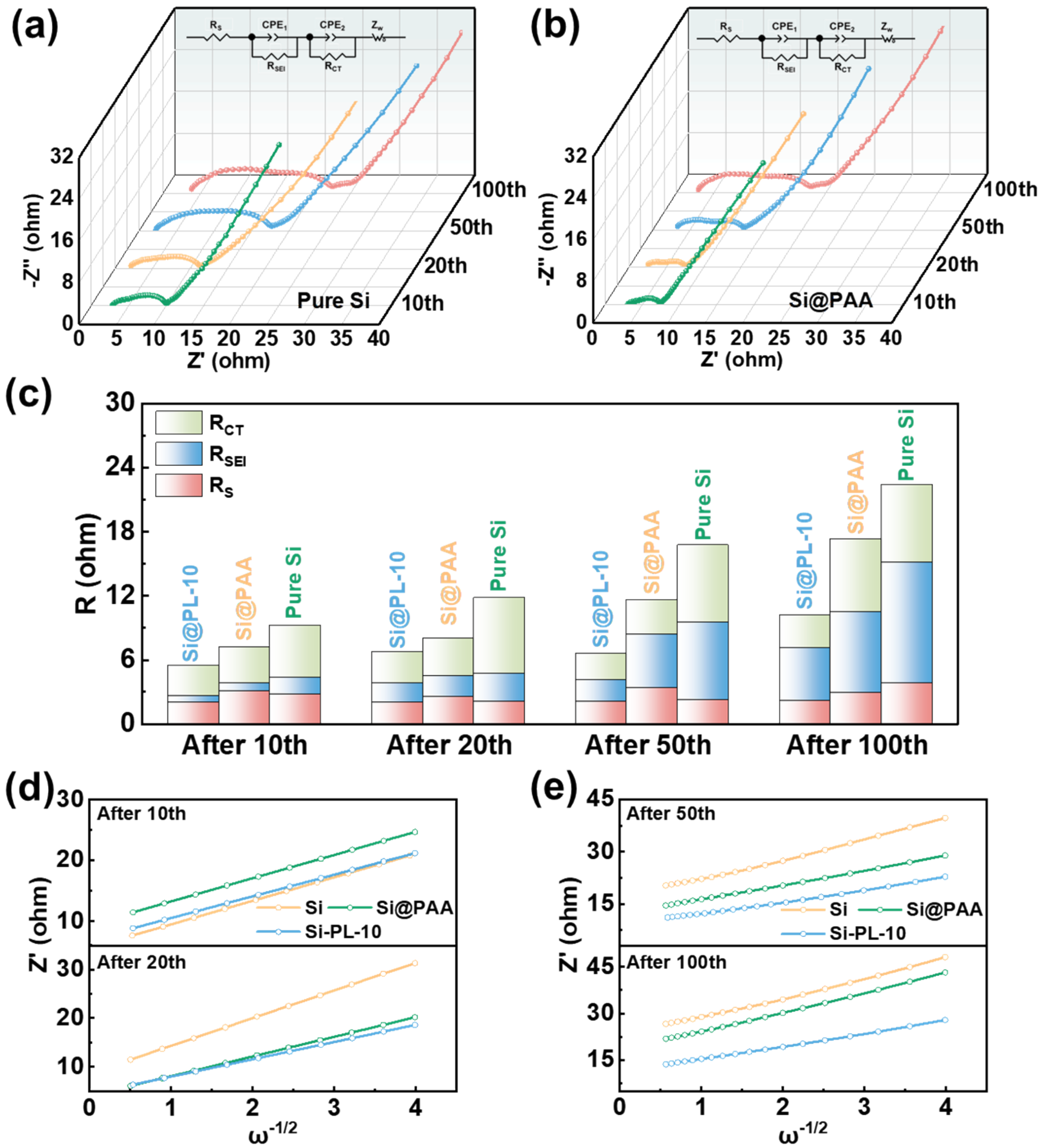

Fig. S5. Nyquist plots of (a) pure Si, (b) Si@PAA electrode after 10, 20, 50, and 100 cycles at 1 A/g. (c) Impedance of different Si electrodes at varied cycles. Warburg impedance plots at low frequency after (d) 10 cycles and 20 cycles and (e) 50cycles and 100 cycles.

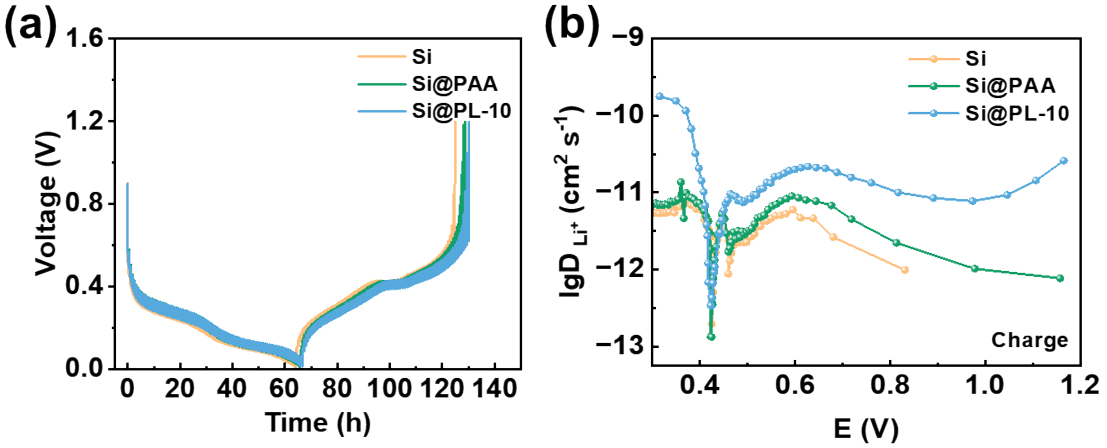

Fig. S6. (a) Galvanostatic intermittent titration technique (GITT) curves of Si@PL-10, Si@PAA and pure Si in both charge and discharge processes. (b) The Li-ion diffusion coefficients (D_{Li^+}) during the charge process calculated from the GITT profile.

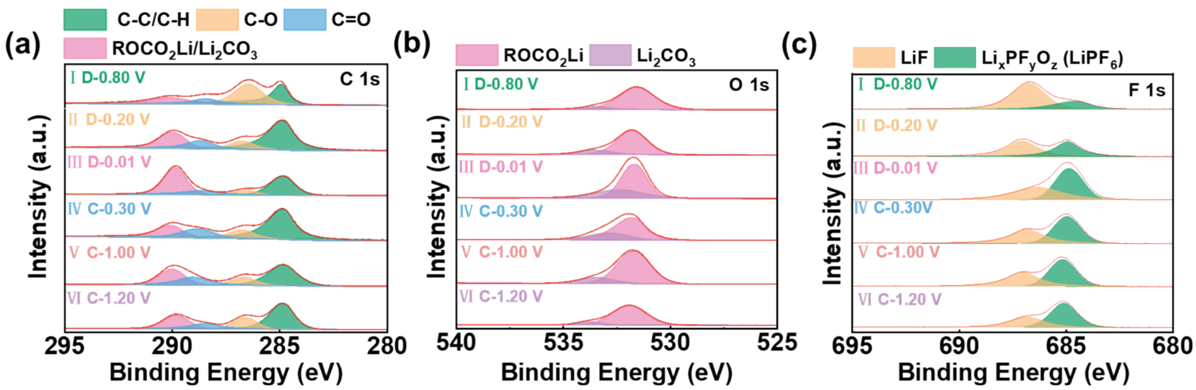

Fig. S7. Ex-situ XPS spectra of the Si@PL-10 electrode on the initial cycle. (a) C 1s spectra, (b) O1s spectra, (c) F 1s spectra.

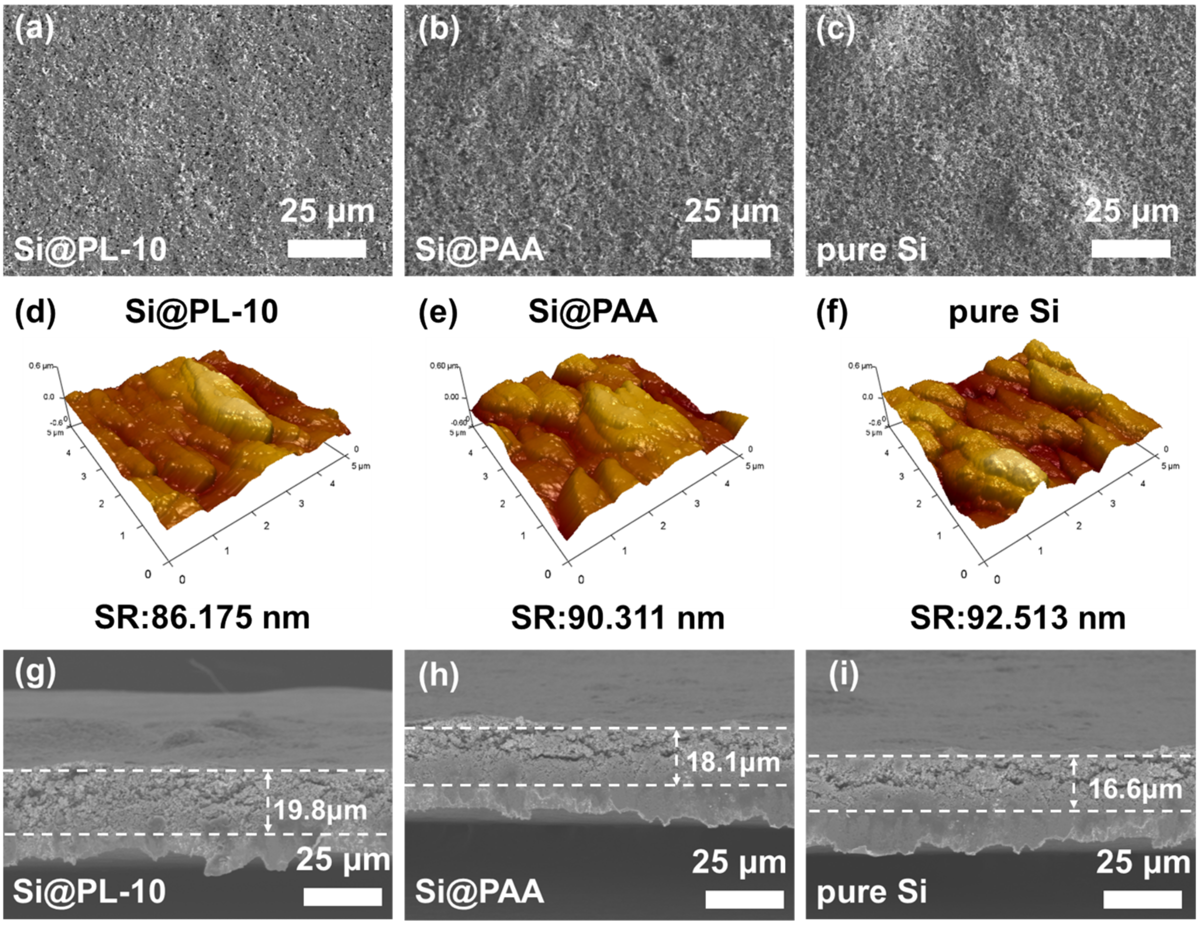

Fig. S8. Top-viewed SEM images of various Si electrodes before cycling. (a) Si@PL-10, (b) Si@PAA, and (c) pure Si. AFM images of surface morphology of various Si electrodes before cycling. (d) Si@PL-10, (e) Si@PAA, and (f) pure Si. Cross-sectional SEM images of various Si electrodes before cycling. (g) Si@PL-10, (h) Si@PAA, and (i) pure Si.

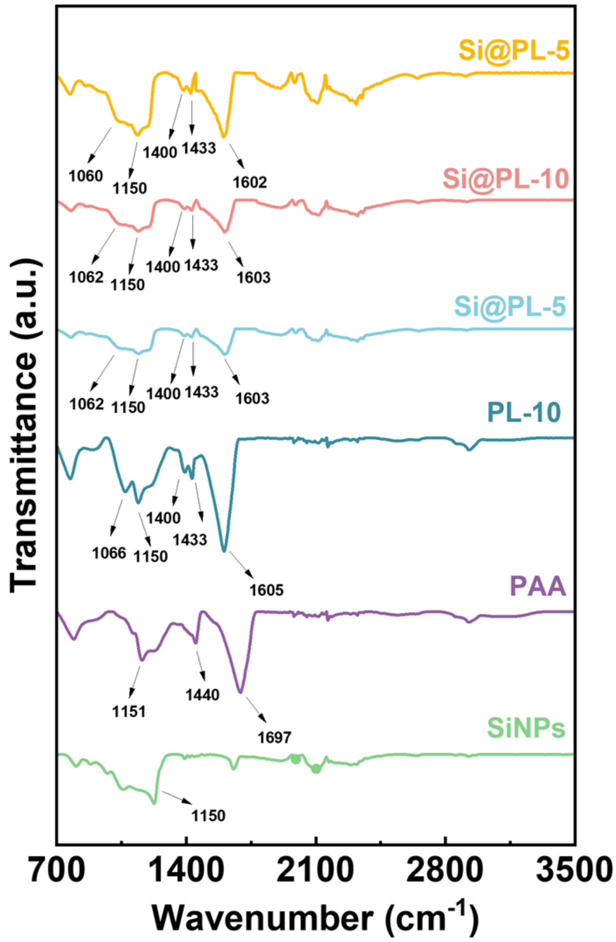

Fig. S9. FTIR spectra of the SiNPs, PAA, PL-10, Si@PL-5, Si@PL-10 and Si@PL-15

$$D_{Li^+} = \frac{R^2T^2}{2A^2n^4F^4C^2\sigma^2} \quad (1)$$

Equation S1. Where R is the gas phase constant, T is room temperature, A is the surface area of the electrode, n (1) is the charge transfer number, F is the Faraday constant (9.6486×10^4), C is the Li^+ concentration in the Si electrode, σ is the Warburg coefficient, which is the slope of the lines depicted in $\omega^{-1/2}$-Z'.

$$D_{Li^+} = \frac{4}{\pi\tau}\left(\frac{n_M V_M}{S}\right)^2\left(\frac{\Delta E_s}{\Delta E_\tau}\right)^2 \quad (2)$$

Equation S2. where τ represents the pulse time (600 s), n_M is the number of moles, V_M is the molar volume of the active material, S stands for the electrode-electrolyte contact area (1.13 cm^{-2}), ΔE_S is the potential change at the end of two subsequent relaxation periods, ΔE_τ represents the potential change during the current pulse.[1]

Table S1. The corresponding resistance [ohm] results obtained by fitting to the circuit.

		Si@PL-10	Si@PAA	Pure Si
10th	R_S	2.078	3.089	2.827
	R_{SEI}	0.579	0.785	1.569
	R_{CT}	2.842	3.313	4.84
20th	R_S	2.06	2.588	2.144
	R_{SEI}	1.754	1.945	2.578
	R_{CT}	2.956	3.467	7.125
50th	R_S	2.137	3.359	2.262
	R_{SEI}	1.998	5.084	7.255
	R_{CT}	2.499	3.218	7.249
100th	R_S	2.192	2.944	3.821
	R_{SEI}	4.94	7.547	11.35
	R_{CT}	3.069	6.851	7.243

Table S2. The calculated D_{Li^+} [cm^2 s^{-1}] from electrochemical impedance analysis.

Electrode	10th	20th	50th	100th
Si@PL-10	6.03E-12	6.1E-12	6.67E-12	4.58E-12
Si@PAA	5.27E-12	4.71E-12	4.47E-12	2.12E-12
Pure Si	5.13E-12	2.38E-12	2.39E-12	2E-12

Table S3. A comparison of cycle stability and rate performance between the Si@PL-10 electrode and the other representatively reported Si anodes for LIBs.

Materials	Cycle stability (mAh g^{-1})		Rate performance (mAh g^{-1})	Ref.
Si@PL-10	**1.0 A g^{-1} 2297 (200th)**	**4.0 A g^{-1} 1978 (100th)**	**6.0 A g^{-1} 1905**	**This work**
SiO_x/C@void@Si/C	0.20 A g^{-1} 1094 (550th)	5.0 A g^{-1} 351 (2000th)	5.0 A g^{-1} 450	2
B-3DCF/Si@C	0.40 A g^{-1} 1288.5 (600th)	1.0 A g^{-1} 1084.3 (800th)	2.0 A g^{-1} 988	3
Si@TTFPB 3%	0.84 A g^{-1} 1778.7 (500th)	/	42 A g^{-1} 1869.4	4
Si@PP	1.0 A g-1 1295 (300th)	4.0A g^{-1} 1718 (60th)	8.0 A g^{-1} 1333	5
Si@PP@CA	0.2 A g^{-1} 2530 (100 th)	1 A g^{-1} 1590 (100 th)	3.2 A g^{-1} 1606	6
Si@NC@SnO_2	0.3 A g^{-1} 1056 (200th)	2 A g^{-1} 510.7 (100th)	2 A g^{-1} 764.1	7
Si@void@meso–C	0.42 A g^{-1} 1250 (100 th)	0.42 A g^{-1} 1250 (150 th)	4.2 A g^{-1} 720	8
Si@SA@Borax	0.5 A g^{-1} 1655.8 (500th)	/	/	9
Si@FG/C	0.2 A g^{-1} 510 (100 th)	0.2 A g^{-1} 500 (150 th)	5 A g^{-1} 200	10
Si@C core–shell nanocomposite	1.26 A g^{-1} 1040 (100 th)	1.26 A g^{-1} 1030 (150 th)	/	11

Si@C	2.1 A g^{-1} 1150 (100 th)	/	/	12
Si@10C	0.5 A g^{-1} 1500 (150 th)	/	/	13
si@AC/OC	0.36 A g^{-1} 1250 (150 th)	/	7.2 A g^{-1} 200	14
H-SiLC-2	1 A g^{-1} 1250 (150 th)	2 A g^{-1} 1240 (100 th)	5 A g^{-1} 1200	15
Si@CMR	0.4 A g^{-1} 1700 (120 th)	/	2 A g^{-1} 1400	16
Si@PANI/SPA	1.2 A g^{-1} 1500 (100 th)	/	4 A g^{-1} 250	17
Si@SiO2@C	1 A g^{-1} 800 (100 th)	/	/	18
Si-NP@	0.3 A g^{-1} 1000 (150 th)	/	1.6 A g^{-1} 900	19
SiNP@CT	/	/	8 A g^{-1} 650	20

References

1. A. A. Cardenas, N. Herlin-Boime, C. Haon and L. Monconduit, *Electrochimica Acta*, 2024, **475**, 143691.
2. W. Chen, S. Kuang, H. Wei, P. Wu, T. Tang, H. Li, Y. Liang, X. Yu and J. Yu, *Journal of Colloid and Interface Science*, 2022, **610**, 583-591.
3. J. Zhao, B. Wang, Z. Zhan, M. Hu, F. Cai, K. Świerczek, K. Yang, J. Ren, Z. Guo and Z. Wang, *Journal of Colloid and Interface Science*, 2024, **664**, 790-800.
4. Z. Cao, X. Zheng, Y. Wang, W. Huang, Y. Li, Y. Huang and H. Zheng, *Nano Energy*, 2022, **93**, 106811.
5. K. Wang, H. Li, X. Chen, Z. Wan, T. Wu, W. Ahmad, D. Qian, X. Wang, J. Gao and R. Khan, *Small Methods*, 2024, **8**, 2301667.
6. B. Chen, D. Xu, S. Chai, Z. Chang and A. Pan, *Advanced Functional Materials*, 2024, **34**, 2401794.
7. K. Tian, X. Li, Q. Zhou, Z. Song, C. Guan, S. Zhuang, M. Zhang and M. Lu, *ACS Sustainable Chemistry Engineering*, 2024, **12**, 959-969.
8. J. Yang, Y.-X. Wang, S.-L. Chou, R. Zhang, Y. Xu, J. Fan, W.-x. Zhang, H. Kun Liu, D. Zhao and S. Xue

Dou, *Nano Energy*, 2015, **18**, 133-142.
9. T. He, Y. Ding, H. Zhang, C. Liu, X. Lou, S. Zhu, X. Yang, L. Yang and H. Bai, *ACS Sustainable Chemistry Engineering*, 2025, **13**, 4093-4107.
10. H. Wang, J. Xie, S. Zhang, G. Cao and X. Zhao, *RSC Advances*, 2016, **6**, 69882-69888.
11. Z. Lu, B. Li, D. Yang, H. Lv, M. Xue and C. Zhang, *RSC Advances*, 2018, **8**, 3477-3482.
12. W. Tan, F. Yang, Z. Lu and Z. Xu, *ACS Applied Energy Materials*, 2022, **5**, 12143-12150.
13. W. Luo, Y. Wang, S. Chou, Y. Xu, W. Li, B. Kong, S. X. Dou, H. K. Liu and J. Yang, *Nano Energy*, 2016, **27**, 255-264.
14. G. Fang, X. Deng, J. Zou and X. Zeng, *Electrochimica Acta*, 2019, **295**, 498-506.
15. J. Shi, H. Gao, G. Hu and Q. Zhang, *Energy Storage Materials*, 2022, **44**, 239-249.
16. Q. Ma, H. Xie, J. Qu, Z. Zhao, B. Zhang, Q. Song, P. Xing and H. Yin, *ACS Applied Energy Materials*, 2020, **3**, 268-278.
17. H.-Y. Lin, C.-H. Li, D.-Y. Wang and C.-C. Chen, *Nanoscale*, 2016, **8**, 1280-1287.
18. Y. Zhang, B. Li, B. Tang, Z. Yao, X. Zhang, Z. Liu, R. Gong and P. Zhao, *Journal of Alloys and Compounds*, 2020, **846**, 156437.
19. X. Zhou, Y.-X. Yin, L.-J. Wan and Y.-G. Guo, *Advanced Energy Materials*, 2012, **2**, 1086-1090.
20. H. Wu, G. Zheng, N. Liu, T. J. Carney, Y. Yang and Y. Cui, *Nano Letters*, 2012, **12**, 904-909.